GEOPOLYMERS FROM NATURAL KAOLIN: ASSESSMENT OF SYNTHETIC CONDITIONS AND MECHANICAL-MICROSTRUCTURAL CHARACTERIZATION

ELISA GASPARINI

Dipartimento di Scienze della Terra e dell'Ambiente, Università di Pavia, Via Ferrata 1, 27100 Pavia

INTRODUCTION AND AIMS

Inorganic aluminosilicate polymers, or geopolymers, are alkali-activated binders with potential use in many application fields, in particular as high-performance, environmental-friendly materials for structural applications and possible replacement for ordinary Portland cement.

The first studies of alkali-activation techniques were conducted in the beginning of the 1940s (Feret, 1939; Purdon, 1940). Only at the end of the 1970s the term geopolymer first appeared to define all types of alkali- or alkali-silicate-activated aluminosilicate materials and to emphasize their similarities with the three dimensional silico-aluminate structures of natural tectosilicate minerals, like feldspathoids and zeolites (Davidovits, 1979, 1989, 1991). Geopolymer network consists of SiO_4 and AlO_4 tetrahedra linked alternately by sharing all oxygen atoms. To maintain the charge neutrality of the polymeric system, the negative charge deriving from Al^{3+} substituting Si^{4+} in tetrahedral coordination is balanced by alkali cations like Na^+, K^+ or Ca^{2+} in the framework cavities. The resulting general empirical formula is $M_n[-(SiO_2)_z-AlO_2]_n \cdot wH_2O$, where M is the alkali cation, n is the degree of polymerization and z usually varies from 1 to 3.

However, contrarily to tectosilicates, geopolymers are the product of the transformation of a solid aluminosilicates source into an amorphous alkali-aluminosilicate material, even though some authors have recognized different degrees of crystallinity of the polymeric gel (*e.g.*, Xu & van Deventer, 2002; Yip *et al.*, 2003; Kriven *et al.*, 2004; Provis *et al.*, 2005; Wang *et al.*, 2005). Several reactions have been recognised to occur during the geopolymerization process; according to Duxson *et al.* (2007a), they can be mainly summarised as follows: dissolution of the aluminosilicate precursor by alkaline hydrolysis; incorporation in the aqueous phase of the species released by raw material dissolution producing a complex mixture of aluminate, silicate and aluminosilicate species which can undergo to gelation (releasing water); reorganization of the gel until the formation of an amorphous three-dimensional aluminosilicate network. Because of the strong competitiveness among different reaction pathways and their possible simultaneous occurrence, it is difficult to achieve a full control of each process involved in geopolymer formation and, therefore, of the properties of synthesis products.

Depending on the raw material and processing conditions, geopolymers can exhibit a wide variety of properties and characteristics, such as high compressive strength, rapid controllable setting and hardening, fire resistance up to 1000 °C with no emission of toxic fumes when heated, resistance to a range of different acids and salt solutions, low shrinkage and low thermal conductivity, adhesion to fresh and old concrete substrates, steel, glass and ceramics, high surface definition that replicates mould patterns (Duxson *et al.*, 2007b, and references therein). Not all geopolymers possess all of these properties, but as in all material technologies the final goal is to ultimately tailor processing conditions, recipes and formulations to achieve required specifications. Commonly, the success of geopolymerization is evaluated by measurement of the compressive strength of synthesised samples. This approach is due to the low cost and the simplicity of the test, and to the importance of strength development in several geopolymers applications (Provis *et al.*, 2005). The compressive strength of geopolymers depends on a number of factors including type and nature of the starting materials, the type of the alkaline cation, the SiO_2/Al_2O_3 and M_2O/H_2O ratios of the synthesised polymer and its maturation conditions, such as curing regime (temperature and time) plus a second thermal treatment performed after curing, also called oven drying (see Komnitsas & Zaharaki, 2007, for a review). The maturation conditions can control the amorphous nature of geopolymers, its degree of crystallinity and its texture/microstructure, the polymeric gel strength and the ratio of the gel phase/undissolved Al-Si particles. Even though numerous studies have

investigated the effect of geopolymer composition on their properties (*e.g.*, Rowles & O'Connor, 2003; He *et al.*, 2012), few studies dealt with the effect of curing regime on the geopolymerization process and/or compressive strength and texture of metakaolin-based polymers (Alonso & Palomo, 2001; Cioffi *et al.*, 2003; Perera *et al.*, 2007; Rovnaník, 2010; Muñiz-Villarreal *et al.*, 2011; Burciaga-Diaz *et al.*, 2012; Arrelano-Aguilar *et al.*, 2014; Cai *et al.*, 2014). In general, results published in various articles cannot be easily compared due to the difference in metakaolin precursors and the large number of processing variables that are different from study to study. Nonetheless, considering the compressive strength values reported in literature for these samples, the geopolymers strength varies largely from as low as 7 to as high as 75 MPa. Curing at temperatures above ambient is reported to favour the development of high compressive strength (Barbosa *et al.*, 2000; Rowles & O'Connor, 2003; Alonso & Palomo, 2001; Perera *et al.*, 2007; Rovnanik, 2010), but other authors report instead better results at room temperature (Burciaga-Diaz *et al.*, 2012; Arellano-Aguilar *et al.*, 2014). These results have demonstrated that one of the major drawbacks in geopolymer research is not only the lack of a standardized experimental composition but also of processing technique.

Accordingly, the main purpose of this work is to investigate the influence of different maturation conditions (curing step and oven drying procedure) on compressive strength and linear shrinkage of geopolymers of fixed composition synthesised by using an industrial kaolin precursor. To achieve this aim, a systematic study has been applied: *i*) the geopolymer synthesis has been performed by following a statistical approach; *ii*) compressive strength measurement have been used as qualitative tool to assess the success of synthesis reaction; *iii*) a petrographic approach has been applied to study the textural features of synthesised samples from the macroscopic to the microscopic scale. A characterization of all geopolymer elements, like aluminosilicate gel phase, un-reacted particles, non-reactive phases and new precipitated phases, is here proposed. According to maturation conditions, the relationships among geopolymer constituents have been investigated and their influence on geopolymers mechanical properties have been elucidated.

The kaolin used for the synthesis has been firstly characterised and the study of the thermal dehydroxylation/amorphization process of kaolinite has been carried out. The kinetic parameters of the process have been determined by performing ex situ thermal treatments of kaolin and characterising the heat treated samples by using a multi-technique approach including sample mass loss, X-ray Power Diffraction (XRPD) and Fourier Transform - Infrared Attenuated Total Reflectance (FTIR-ATR) spectroscopy. The Design of Experiment (DoE) method has been used to study the influence of temperature of curing (x_1), time of curing (x_2) and oven drying after curing (x_3) variables on compressive strength and linear shrinkage of polymers through a face-centered cubic design (FCC). Compared with the "one-variable-at-a-time" method, the FCC regression model allowed us to estimate the effect of each variable, their linear interactions and their quadratic effects on the responses analysed by a multiple linear regression (Alvarez-Ayuso *et al.*, 2008). The geopolymers have been characterized by using a combination of experimental techniques, such as XRPD, FTIR-ATR, optical and scanning electron microscopy (OM and SEM respectively), differential thermal analysis (DTA) and gas pycnometry.

MATERIALS AND METHODS

Kaolin characterization

A German industrial kaolin, labelled Sl-K, provided by Sibelco Italia S.p.A has been used for the present study. The chemical composition of this raw material, determined by X-ray fluorescence (XRF) methods, is: SiO_2 67.0 wt.%, Al_2O_3 31.5 wt.%, Fe_2O_3 0.32 wt.%, TiO_2 0.24 wt.%, CaO 0.12 wt.%, MgO 0.23 wt.%, and K_2O 0.35 wt.%, and its measured loss on ignition is 10.02%. The XRPD pattern of Sl-K sample shows only the characteristic reflections of kaolinite and quartz. However, according to XRF data, others mineral phases, such as mica or feldspar group minerals, iron oxides (as hematite) and titanium dioxide (as rutile), could be also present. These impurities, due to their small amount, are not detectable by using XRPD technique.

According to thermogravimetric (TG) analyses, kaolin has a mass loss of *ca.* 9.5% due to the dehydroxylation of kaolinite and formation of metakaolinite. The mass loss data has been used to roughly estimate the content of kaolinite in Sl-K sample to *ca.* 73%. According to DTA analyses, the dehydroxylation reaction occurs as a strong endothermic valley peaked at 528 °C, while at 1009 °C mullite is formed.

The kaolin average particle size distribution was measured by a Sympatec Helos particle size analyser equipped with a laser diffraction sensor and resulted of *ca.* 3 μm for kaolinite and of *ca.* 10 μm for quartz.

The annealing experiments were performed *ex situ* at four different temperatures: 450, 500, 550 and 600 °C, using a vertical furnace Carbolite STF 15/450. At each working temperature, different heating times were used in order to monitor the evolution of the dehydroxylation process to the end of the reaction. Each heated sample has been characterised by measuring its initial and final mass and the corresponding water loss and the intensities of (001) peak of kaolinite normalized with respect to (101) peak of quartz obtained by diffraction patterns. Furthermore, it is here proposed to study the amorphisation process by analyzing the evolution of the average linewidth of the Si-O and Al-O stretching modes region of IR spectra with annealing time. In particular, the spectral range from 670 to 2000 cm^{-1} has been analysed by applying an autocorrelation approach (Salje *et al.*, 2000). The instrumental details, all sequence of thermal treatments and measured parameters of each experiment are reported in Gasparini *et al.* (2013).

Geopolymer synthesis and characterization

Geopolymers were synthesized by mechanically mixing the thermally activated (at 550 °C for 3 hours) Sl-K powder with the alkaline solution for 5 minutes. The powder-to-liquid ratio was stoichiometrically determined to allow the following molar oxide ratios formulation of the synthesised samples: $SiO_2/Al_2O_3 = 4.6$, $(Na_2O+K_2O)/SiO_2 = 0.3$, $Al_2O_3/(Na_2O+K_2O) = 1$, and $H_2O/(Na_2O+K_2O) = 12$. It is also important to note that the SiO_2/Al_2O_3 ratio was calculated on the basis of the actual metakaolinite product as determined on the basis of TG analysis.

Once the synthesis procedure has been concluded, the mixture has been poured into two different types of cylindrical Teflon moulds: one having size 2 cm diameter (Ø), 4 cm height (h), suitable for compressive strength tests; the other being Ø = 2.54 cm, h = 2 cm, used for the measurement of the linear shrinkage. The slurry was poured into the moulds and subjected to the maturation phase defined by considering the different maturation conditions reported in literature for metakaolin-based geopolymers (*e.g.*, Duxson *et al.*, 2007b; Rovnanik, 2010; Heah *et al.*, 2011; Burciaga-Diaz *et al.*, 2012). A total number of 18 experiments were defined by the FCC design (Table 1): the samples were cured in a laboratory oven at three different temperatures, 40, 65 or 90 °C and, for each temperature three different curing times, 1, 9 or 19 hours, were used.

During this maturation step the moulds were sealed at their tops using a polyethylene film to retain the water inside the system and finally opened at the end of the curing. All these conditions were used with or without a final oven drying treatment at 60 °C for 24 hours. According to DoE method, the upper and lower limits of each studied variable temperature, time and drying (x_1, x_2, x_3 respectively) define the experimental domain (Box, 1951), in which the variation of the analysed responses, compressive strength and linear shrinkage, has been studied. For each of the eighteen synthesized samples, two replicates were performed to test the variability of compressive strength measurements; all the measured values were considered in the statistical analyses. In addition, three more replicates were performed for the response Y_1 at the central level of the x_1 and x_2 variables without oven drying to better study the response surface model behaviour at these conditions. The reliability of model prediction was tested by performing one experiment, called validation experiment, with two independent replicates, for both the analysed responses. Data analysis was performed using Matlab in-house routines provided by Prof. Riccardo Leardi (University of Genova, Italy).

The compressive strength was tested by using an unconfined uniaxial Metrocom compressive machine with a 5000 kg loading cell and a loading rate of 50 kg·sec^{-1} at the Dipartimento di Ingegneria Civile ed Architettura, University of Pavia. The samples were tested after 28 days of ageing, starting from the end of the maturation treatment, according to ASTM C39-96 (ASTM C39-96, 1999). The linear shrinkage was obtained by

measuring the linear change in lower diameter of each cylindrical synthesized sample after 28 days from the end of the maturation phase, by using a micrometer. The compressive strength and linear shrinkage values measured from the polymers are reported in Table 1.

Table 1 - Designed experiments according to Face Centered Design for the optimization of compressive strength (Y_1) and linear shrinkage (Y_2) of metakaolin-based geopolymers.

Experiment No.	Experimental matrix			Experimental plan			Y_1 Measure (MPa)			Y_2 Measure (%)		
	x_1	x_2	x_3	X_1	X_2	X_3	1	2	3	1	2	3
1	40	1	Yes	-1	-1	1	45	38	35	1.9	-	-
2	90	1	Yes	1	-1	1	38	33	44	3.8	-	-
3	40	19	Yes	-1	1	1	56	44	45	2.0	-	-
4	90	19	Yes	1	1	1	15	15	15	6.4	-	-
5[a]	40	1	No	-1	-1	-1	11	-	-	5.8	-	-
6	90	1	No	1	-1	-1	27	32	39	8.4	-	-
7	40	19	No	-1	1	-1	74	78	72	1.6	-	-
8	90	19	No	1	1	-1	10	11	10	5.4	-	-
9	65	9	Yes	0	-0.1	1	53	48	48	1.2	-	-
10[b]	65	9	No	0	-0.1	-1	51	51	52	1.4	-	-
11	90	9	Yes	1	-0.1	1	34	36	29	5.4	-	-
12	40	9	Yes	-1	-0.1	1	50	44	53	3.3	-	-
13	90	9	No	1	-0.1	-1	33	23	31	3.7	-	-
14	40	9	No	-1	-0.1	-1	32	31	27	3.3	-	-
15	65	19	Yes	0	1	1	54	44	54	0.7	-	-
16	65	1	Yes	0	-1	1	51	36	48	1.7	-	-
17	65	19	No	0	1	-1	59	52	58	0.4	-	-
18	65	1	No	0	-1	-1	65	69	79	6.7	-	-
	vx_1	vx_2	vx_3	VX_1	VX_2	VX_3						
Validation Experiments	52.5	17.12	No	-0.5	0.8	0.1	67	61	63	0.5	0.5	0.7

The natural variables (temperature, x_1; time, x_2; oven drying, x_3), scaled values (X_1; X_2; X_3) and related experimental matrix and experimental plan are reported. Temperature, time and oven drying condition of validation experiments (natural variables: vx_1, vx_2, vx_3; scaled values: VX_1, VX_2, VX_3) and related responses are also indicated. The standard deviation calculated from compressive strength and linear shrinkage values measured from validation samples are 3 and 0.1, respectively. The confidence interval (probability = 0.95) calculated is 3 for compressive strength and 0.1 for linear shrinkage.

[a] At this experimental condition only one valid measurement was obtained due to the intense fracturing of the other two replicates: consequently these experiments were excluded by the model computation.

[b] Three more replicates were performed for the response Y_1 at these experimental conditions. The measured values are: 55, 55 and 51 MPa.

All the synthesized samples were analysed by using XRPD and FTIR-ATR techniques. The texture of selected samples, obtained at different curing conditions, has been studied at different length scale by using a stereoscopic microscope and Field Emission - Scanning Electron Microscope (FE - SEM).

The density and thermal stability of all samples have been analysed by using a helium pycnometer ULTRAPYC 1200e and DTA analyses, respectively.

RESULTS AND DISCUSSION

Kinetic of dehydroxylation of kaolinite of Sl-K kaolin has been investigated at 450, 500, 550 and 600 °C, by using the Avrami method (Avrami, 1939). For each temperature, the variation with time under isothermal conditions of the following parameters has been studied: *i*) moles of water lost during heating; *ii*) intensity of

$(001)_K$ diffraction peak of kaolinite; *iii*) average linewidth, expressed as Δ_{corr}, of IR bands in the 670 to 2000 cm^{-1} region. According to the results, only datasets relative to T = 500, 550, and 600 °C resulted to be isokinetic, suggesting a change of the kaolinite dehydroxylation mechanism at 450°C. This is in accordance with what reported in previous works (Redfern, 1987; Bellotto *et al.*, 1995). In the temperature range 500-600 °C, the activation energy associated to the process, as determined on the basis of the three measured parameters, is: 137 ± 19 kJ mol^{-1} (R = 0.99) from mass loss, 139 ± 22 kJ mol^{-1} (R = 0.987) from intensity of XRPD peaks, 127 ± 38 kJ mol^{-1} (R = 0.959) from intensity of IR bands. Such values are very similar, indicating that the three parameters give a direct response to the degree of metakaolinitization of kaolinite. The activation energy values determined in this work are in the lower limit but within the range of previously published data (Bellotto *et al.*, 1995; Dion *et al.*, 1998; Ortega *et al.*, 2010).

A high variability of compressive strength and linear shrinkage values, measured on synthesised metakaolin-based geopolymers of fixed composition, were observed with different maturation conditions (Table 1). The compressive strength values ranged from 10 to 79 MPa. The lowest values were obtained for the samples synthesized at the boundaries of the experimental domain, *i.e.*, 90 °C for 19 hours and 40 °C for 1 hour, without oven drying process. In contrast, the largest strength were achieved by curing at 40 °C for 19 hours or at 65 °C for 1 hour, without drying procedure. Instead, the polymers linear shrinkage ranged from 0.4 to 8.4%. Geopolymers characterized by low shrinkage values were obtained at 65 °C for 19 hours with or without drying, whereas the linear shrinkage values higher than 3.7% were measured for all the samples cured at 90 °C. In particular, at this temperature the largest shrinkage (8.4%) was obtained by curing for 1 hour without oven drying the polymer sample. If short curing times without oven drying procedure were applied, elevated linear shrinkage were also measured for the samples synthesized both at 40 °C (5.9%) and 65 °C (6.7%). As regards the effect of the oven drying, by considering both the analysed responses, it is clear that for this procedure it is necessary to improve the mechanical and physical performances of the geopolymers only in the case of short curing time (1 hour) experiments.

Statistical analysis of the compressive strength and linear shrinkage data set has allowed to find the significant terms influencing the studied responses. By considering the compressive strength data for samples given in Table 1, the following significant terms have been calculated: *i*) temperature (probability, $p < 0.001$); *ii*) interaction temperature-time ($p < 0.001$); *iii*) square term for temperature ($p < 0.001$). The fraction of the total variance explained in cross validation is 59%. The significant terms influencing linear shrinkage are: *i*) temperature ($p < 0.01$); *ii*) time ($p < 0.05$); *iii*) interaction time-drying ($p < 0.01$); *iv*) square term for temperature ($p < 0.01$). In this case, the explained variance cross validated for the model is 40%. The validation of the model was performed at the maturation condition of the validation experiments reported in Table 1. The predicted responses are 62 MPa and 0.5% for compressive strength and linear shrinkage, respectively; which are actually very close to the average of the experimental values (see Table 1). Therefore, the model can be used to predict the studied responses in the all experimental domain.

The response surfaces and contour lines of temperature *vs.* time, obtained by statistical analysis of the data set obtained without drying procedure, are reported in Fig. 1a-b for the two responses. It had been shown in fact that the oven drying procedure only improves the quality of synthesised geopolymers cured for short times. In both cases the drying parameter has therefore been set equal to -1 (meaning without oven drying). From Fig. 1a, it is clear that the largest compressive strength values are obtained at temperatures between 40 and 60 °C for long curing times; whereas the lowest shrinkage are obtained at relatively low temperatures (between 45 and 65 °C) if long curing times are used (> 16 hours; Fig. 1b). Considering the experimental domain, the optimum condition to synthesise geopolymers characterised by the largest compressive strength and lowest linear shrinkage can be easily determined: a compressive strength of 65 MPa is obtained for a curing procedure at 49.5 °C for 19 hours, whereas the lowest shrinkage (0.2 %) is obtained for 19 hours of curing at about 57.5 °C.

According to XRPD analyses, the geopolymers synthesised under different maturation conditions have revealed the same phase composition. All diffractograms show the presence of quartz, residual kaolinite, which

is due to the low temperature (550 °C) used for kaolin activation, and a broad "hump" centred at *ca*. 27-29 °2θ. This last signal corresponds to the distinguishing feature of the amorphous aluminosilicate phase formed during polymerization reaction.
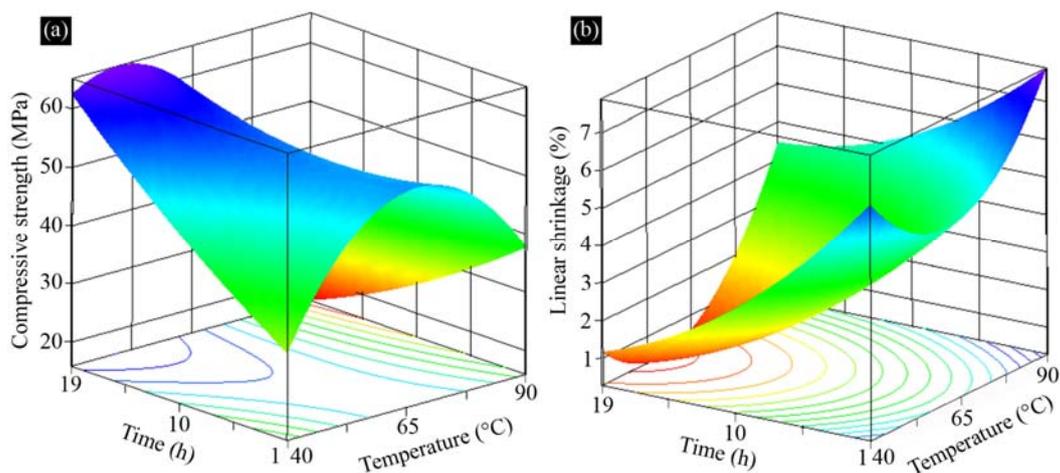

Fig. 1 - The response surfaces and contour lines of temperature *vs*. time without oven drying procedure predicted on the basis of FCC model equation for the two analysed responses, compressive strength (a) and linear shrinkage (b).

All FTIR-ATR spectra collected from grounded and washed geopolymer pieces resulted after mechanical tests have shown a broad band centered at about 1003 cm^{-1}. This band is related to asymmetric stretching of the Si-O-T bonds, where T is Si or Al in tetrahedral coordination (Rees *et al.*, 2007), and it is considered as a major fingerprint for the aluminosilicate gel. Its position depends on the extent of aluminium incorporation and/or network structure (Rees *et al.*, 2007). In this work, the position of this Si-O-T band is the same for all samples revealing, therefore, a similar average chemical composition among all synthesised geopolymers. High frequency bands at 3480 and 1625 cm^{-1}, related to O-H stretching group and bending modes of molecular water respectively, are also present. This indicates the presence of OH groups linked to the structure, but also of water molecules which are adsorbed on the surface or entrapped in the large cavities of the geopolymer framework (Fernandez-Jimenez & Palomo, 2005).

The spectra collected directly from geopolymer samples have also revealed peaks at frequencies around 1400 cm^{-1} which are diagnostic of the presence of $(CO_3)^{2-}$ (asymmetric stretching; see Farmer, 1974, for reference) and are therefore indicative of the formation of sodium carbonates as secondary products in the synthesis. In particular, in the sample cured at high temperature (*i.e.*, 90 °C) a peak centered at about 1470 cm^{-1} is predominant. It can be ascribed to the presence of sodium carbonate hydrates such as trona, $Na_3(HCO_3)(CO_3)\cdot2H_2O$, and thermonatrite, $Na_2CO_3\cdot H_2O$, which have already been observed as efflorescence in geopolymers (Komnitsas & Zaharaki, 2007). Instead, the samples cured at low temperatures (*i.e.*, 40 °C and 65 °C) are mainly characterized by the presence in the $(CO_3)^{2-}$ region of IR bands reliable to hydrated double carbonate such as dawsonite, $NaAlCO_3(OH)_2$, suggesting a precipitation reaction, which requires aluminum ions available in solution, or alternatively as a mineral replacement reaction which is however fluid mediated during geopolymer formation.

Fig. 2 shows the stereo-microscope photos (Fig. 2a-c), and related SEM micrographs of the aluminosilicate gel (Fig. 2a 1-3; Fig. 2b 1-3; Fig. 2c 1-3) in the fracture surface of the following samples: S1h40ND (Fig. 2a; cured at 40 °C for 1 hour), S17h52ND (Fig. 2b; cured at 52.5 °C for 17 hours and 12 minutes), S19h90ND (Fig. 2c; cured at 90 °C for 19 hours). These geopolymers differ significantly in the measured values of compressive strength and linear shrinkage.

At the macroscopic scale (Fig. 2a-c), structural features common to all samples can be observed: *i*) a white phase, called "binder", which correspond to the aluminosilicate gel; *ii*) grains of different shapes, sizes and colours, called "aggregates", *iii*) pores of various sizes and shapes. A closed porosity can be noticed in the samples. Pores formation can be related to both air bubbles retained in the mixture during synthesis process and the evaporation of part of process water (He *et al*., 2012).
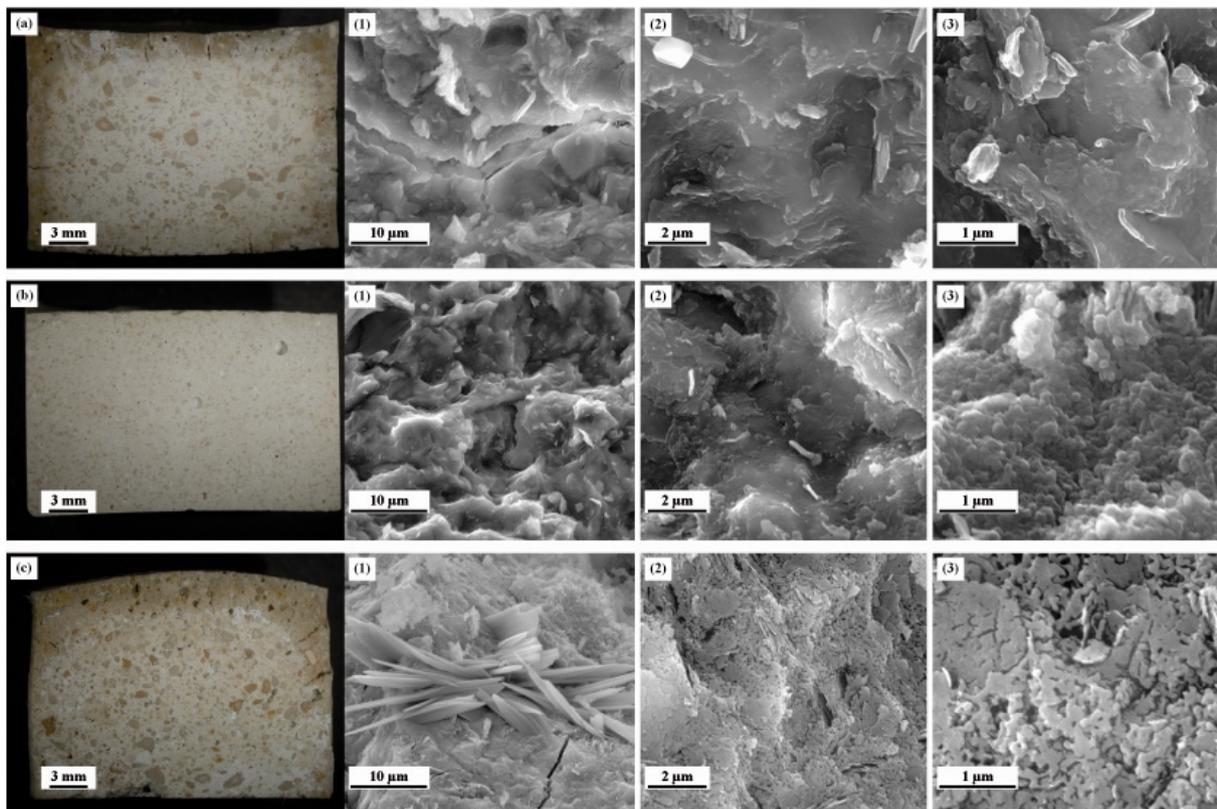

Fig. 2 - Stereo micrograph photos and SEM micrographs of fracture surface of analysed geopolymers: (a) S1h40ND, 11 MPa - 5.8 %; (b) S17h52ND, 67 MPa - 0.5 %; (c) S19h90ND, 15 MPa - 5.4 %. SEM micrographs magnifications are: (1) 5000x; (2) 20000x; (3) 50000x.

A binder phase developed from the inner to the external sample volume characterises the sample S17h52ND (Fig. 2b) which is characterised by the largest compressive strength and lowest linear shrinkage. The aggregates are rounded and equal in size, and homogeneously distributed in the binder, whereas few cavities are dispersed in the aluminosilicate phase. Pore sizes range from 0.5 to 2 mm. With respect to sample S17h52ND, the samples S1h40ND (Fig. 2a) and S19h90ND (Fig. 2c) are characterised by a binder phase which seems to be mainly limited to the inner sample volume, a brown-reddish rim with fractures and large pores (2-3 mm) which are mainly concentrated at the external volume of the geopolymers. As evident from Fig. 2a and c, these samples can be considered as poorly sorted geopolymers, consisting of aggregates, irregular in shape and size, heterogeneously dispersed into the binder. Both samples are low quality geopolymers; they are characterized by low compressive strength and high linear shrinkage. Moreover, as evident from Fig. 2c, the top of the sample S19h90ND has a dome-like shape (Fig. 2c), likely as consequence of fast water evaporation during maturation step, whereas all the other geopolymers are characterised by a flat upper surface.

By comparing the SEM micrographs of fracture surfaces of the three selected samples, textural differences exist among their binder phase, which become more evident by increasing micrographs magnification from 5000x to 50000x. The high-strength sample S17h52ND (Fig. 2b 1) is mainly characterised

by a homogeneous binder phase in which some kaolinite/metakaolinite plates are dispersed. From high resolution images (Fig. 2b 2), it has been possible to recognise that the binder is composed of neo-formed geopolymer "plates" which seem to have increased their size and connectivity during the advancement of the polymerization reaction. At 50000x (Fig. 2b 3), it is evident that each polymer plate has a coarse grained texture made up of aggregates of spherical particles.

The textural features of the other two selected samples (S1h40ND, S19h90ND) are very different from that of the previous one. The sample S1h40ND shows an apparent homogeneous texture at a magnification of 5000x (Fig. 2a 1), even though a layered structure of the binder phase is evident at higher length scale (Fig. 2a 2-3). Each layer is composed by a coarse grained aggregate of spherical polymer particles which seem to grow over and substitute the original metakaolinite plates (Fig. 2a 3). A secondary type of open porosity is also recognizable among the neo-formed geopolymer plates. In this sample, some unreacted metakaolin particles, relicts of the sodium silicate solution employed in geopolymer synthesis, and sodium carbonate crystals can be found within areas dispersed through the binder. Differently, the sample S19h90ND shows a strongly heterogeneous texture (Fig. 2c 1-3). The binder phase is composed of polymeric nano-seed particles (Fig. 2c 2-3), which probably correspond to the first steps of nucleation and growth of binder. These particles are interconnected to form small aggregates, irregular in shape, and, therefore, a strongly nano-porous microstructure characterizes this sample (Fig. 2c 3). Moreover, high amount of unreacted materials, originated from both the metakaolin and sodium silicate solution, are also recognizable in SEM micrographs of fracture surface of this sample (Fig. 2c 1).

Density of geopolymers varies mainly from 2.187 g/cm^3 to 2.326 g/cm^3; whereas porosity data range from 34 to 46%. However, the variations in geopolymers density and porosity seem not to be directly related to their different mechanical strength. The variability of the measured data could be mainly related to pores and fractures developed in samples during maturation step.

According to the results of DTA analyses, the geopolymers are not subjected to crystallization from 40 to 1200 °C and undergo a sintering process at the end of heating.

CONCLUSION

Geopolymer formation requires a complex process and the possibility to obtain homogeneous materials clearly depends on maturation conditions as well as on composition.

The DoE approach can be conveniently used for geopolymer synthesis to recognise which variables affect the properties of products. According to this work, the mechanical behaviour and the linear shrinkage of the metakaolin-based geopolymers of fixed composition depend mainly on temperature and time of curing; their interaction has been shown to strongly influence the quality of synthesised samples. High strength-low shrinkage samples are obtained when long curing time (19 hours) and relatively low curing temperatures (< 65 °C) are applied. At these curing conditions, the drying procedure is demonstrated not to be necessary to improve geopolymer performance. With increasing temperature up to 90 °C, the strength of geopolymers decreases and the shrinkage increases. These results have demonstrated that maturation conditions strongly affect the processes involved during the geopolymerization reaction. In particular, maturation conditions seem to act on the dissolution of aluminosilicate solid precursor and texture of binder phase. Therefore, the choice of geopolymer maturation condition is a fundamental parameter controlling the degree of development and the quality of the aluminosilicate binder which is revealed to be the main factor influencing geopolymer strength.

REFERENCES

Alonso, S. & Palomo, A. (2001): Alkaline activation of metakaolin and calcium hydroxide mixtures: influence of temperature, activator concentration and solids ratio. *Mater. Lett.*, **47**, 55-62.

Alvarez-Ayuso, E., Querol, X., Plana, F., Alastuey, A., Moreno, N., Izquierdo, M. (2008): Environmental, physical and structural characterization of geopolymer matrixes synthesized from coal (co-)combustion fly ashes. *J. Hazard. Mater.*, **154**, 175-183.

Arrelano-Aguilar, R., Burciaga-Dìaz, O., Gorokhovsky, A., Escalante-García, J.I. (2014): Geopolymer mortars based on a low grade metakaolin: Effects of the chemical composition, temperature and aggregate:binder ratio. *Constr. Build. Mater.*, **50**, 642-648.

ASTM C39-96 (1999): Annual Book of ASTM Standards, American Society for Testing and Materials, Philadelphia, PA.

Avrami, M. (1939): Kinetics of phase change. I. General theory. *J. Chem. Phys.*, **7**, 1103-1112.

Barbosa, V.F.F., MacKenzie, K.J.D., Thaumaturgo, C. (2000): Synthesis and characterisation of materials based on inorganic polymers of alumina and silica: sodium polysialate polymers. *Int. J. Inorg. Mater.*, **2**, 309-317.

Bellotto, M., Gualtieri, A., Artioli, A., Clark, S.M. (1995): Kinetic study of the kaolinite-mullite reaction sequence. Part I: kaolinite dehydroxylation. *Phys. Chem. Minerals*, **22**, 207-214.

Box, G.E.P. (1951): The exploration and exploitation of response surfaces: some general considerations and examples. *Biometrics*, **10**, 16-60.

Burciaga-Diaz, O., Escalante-Garcia, J.I., Gorokhovsky, A. (2012): Geopolymers based on a coarse low-purity kaolin mineral: Mechanical strength as a function of the chemical composition and temperature. *Cement Concrete Comp.*, **34**, 18-24.

Cai, B., Mellgren, T., Brendenberg, S., Engqvist, H. (2014): The effect of curing conditions on compressive strength and porosity of metakaolin-based geopolymers. *Develop. Strategic Mater. Comput. Design*, **4,** 49-55.

Cioffi, R., Maffucci, L., Santoro, L. (2003): Optimization of geopolymer synthesis by calcinations and polycondensation of a kaolinitic residue. *Resour. Conserv. Recycl.*, **40**, 27-38.

Davidovits, J. (1979): Synthesis of New High-Temperature Geo-Polymers for Reinforced Plastics/Composites, SPE PACTFC 79, Society of Plastic Engineers, Brookfield Center, USA, 151-154.

Davidovits, J. (1989): Geopolymers and geopolymeric materials. *J. Therm. Anal.*, **35**, 429-441.

Davidovits, J. (1991): Geopolymers - inorganic polymeric new materials. *J. Therm. Anal.*, **37**, 1633-1656.

Dion, P., Alcover, J.F., Bergaya, F., Ortega, A., Llewellyn, P.L., Rouquerol, F. (1998): Kinetic study by controlled-trasformation rate thermal analysis of the dehydroxylation of kaolinite. *Clay Miner.*, **33**, 269-276.

Duxson, P., Fernández-Jiménez, A., Provis, J.L., Lukey, G.C., Palomo, A., van Deventer, J.S.J. (2007a): Geopolymer technology: the current state of the art. *J. Mater. Sci.*, **42**, 2917-2933.

Duxson, P., Provis, J.L., Lukey, G.C., van Deventer, J.S.J. (2007b): The role of inorganic polymer technology in the development of 'green concrete'. *Cement Concrete Res.*, **37**, 1590-1597.

Farmer, V.C. (1974): The infrared spectra of minerals. Mineralogical Society Monograph 4, London, 539 p.

Feret, R. (1939): Slags for the manufacture of cement. Revue des matriaux de construction et de travaux publics, 121-126.

Fernandez-Jimenez, A. & Palomo, A. (2005): Composition and microstructure of alkali activated fly ash binder. Effect of the activator. *Cement Concrete Res.*, **35**, 1984-1992.

Gasparini, E., Tarantino, S.C., Ghigna, P., Ricardo M.P., Cedillo-González, E., Siligardi, C., Zema, M. (2013): Thermal dehydroxylation of kaolinite under isothermal conditions. *Appl. Clay Sci.*, **80-81**, 417-425.

He, J., Zhang, J., Yu, Y., Zhang, G. (2012): The strength and microstructure of two geopolymers derived from metakaolin and red-fly ash admixture: A comparative study. *Constr. Build. Mater.*, **30,** 80-91.

Heah, C.Y., Kamarudin, H., Mustafa Al Bakri, A.M., Bnhussain, M., Luqman, M., Khairul Nizar, I., Ruzaidi, C.M., Liew, Y.M. (2011): Effect of Curing Profile on Kaolin-based Geopolymers. *Phys. Procedia*, **22**, 305-311.

Komnitsas, K. & Zaharaki, D. (2007): Geopolymerization: a review and prospects for the minerals industry. *Miner. Eng.*, **20**, 1261-1277.

Kriven, W.M., Gordon, M., Bell, J.L. (2004): Geopolymers: Nanoparticulate, nanoporous ceramics made under ambient conditions, *In*: "Microscopy and Microanalysis '04". Proc. 62nd Annual Meeting of the Microscopy Society of America), Savannah, GA.

Muñiz-Villarreal, M.S., Manzano-Ramírez, A., Sampieri-Bulbarela, S., Gasca-Tirado, J.R., Reyes-Araiza, J.L., Rubio-Ávalos, J.C., Pérez-Bueno, J.J., Apatiga, L.M., Zaldivar-Cadena, A., Amigó-Borrás, V. (2011): The effect of temperature on the geopolymerization process of a metakaolin-based geopolymer. *Mater. Lett.*, **65**, 995-998.

Ortega, A., Macías, M., Gotor, F.J. (2010): The multistep nature of the kaolinite dehydroxylation: kinetics and mechanism. *J. Am. Ceram. Soc.*, **93**, 197-203.

Perera, D.S., Uchida, O., Vance, E.R., Finnie, K.S. (2007): Influence of curing schedule on the integrity of geopolymers. *J. Mater. Sci.*, **42**, 3099-3106.

Provis, J.L., Lukey, G.C., van Deventer, J.S.J. (2005): Do geopolymers actually contain nanocrystalline zeolites? A reexamination of existing results. *Chem. Mater.*, **17**, 3075-3085.

Purdon, A.O. (1940): The action of alkalis on blast furnace slag. *J. Soc. Chem. Ind.*, **59**, 191-202.

Redfern, S.A.T. (1987): The kinetics of dehydroxylation of kaolinite. *Clay Minerals*, **22**, 447-456.

Rees, C.A., Provis, J.L., Lukey, G.C., van Deventer, J.S.J. (2007): *In situ* ATR-FTIR study of the early stages of fly ash geopolymer gel formation. *Langmuir*, **23**, 9076-9082.

Rovnanik, P. (2010): Effect of curing temperature on the development of hard structure of metakaolin-based geopolymer. *Constr. Build. Mater.*, **24**, 1176-1183.

Rowles, M. & O'Connor, B. (2003): Chemical optimisation of the compressive strength of aluminosilicate geopolymers synthesised by sodium silicate activation of metakaolinite. *J. Mater. Chem.*, **13**, 1161-1165.

Salje, E.K.H., Carpenter, M.A, Malcherek, T., Boffa Ballaran, T. (2000): Autocorrelation analysis of infrared spectra from minerals. *Eur. J. Mineral.*, **12**, 503-519.

Wang, H., Li, H., Yan, F. (2005): Synthesis and mechanical properties of metakaolinite-based geopolymer. *Colloids and Surfaces A: Physicochem. Eng. Aspects*, **268**, 1-6.

Xu, H. & van Deventer, J.S.J. (2002): Microstructural characterisation of geopolymers synthesised from kaolinite/stilbite mixtures using XRD, MAS-NMR, SEM/EDX, TEM/EDX, and HREM. *Cement Concrete Res.*, **32**, 1705-1716.

Yip, C.K., Lukey, G.C., van Deventer, J.S.J. (2003): Effect of blast furnace slag addition on microstructure and properties of metakaolinite geopolymeric materials. *Ceram. Trans.*, **153**, 187-209.